ORIGINAL ARTICLE

The impact of the lanthanide contraction on the structure of complexes of a calix[4]arene trisamide

G. L. Nealon · M. Mocerino · M. I. Ogden · B. W. Skelton

Abstract The syntheses of samarium, holmium, and ytterbium complexes of a tris-amide calix[4]arene are described, and the resulting structures are compared with the previously reported gadolinium complex. The syntheses involved the reaction of 5,11,17,23-tetra-*tert*-butyl-24-hydroxy-26,27,28-tris(diethylcarbamoylmethoxy)calix[4]arene with the appropriate lanthanide picrate hydrate. Structural studies demonstrated that a picrate anion acts as a *quasi*-bidentate ligand with Sm (and Gd), is unidentate in the Ho complex, but is found in the *second* coordination sphere for the smallest lanthanide cation (Yb) investigated.

Keywords Calixarene · Lanthanide · Picrate · Second-sphere coordination

Introduction

Despite the relative maturity of the field, the development of functionalised calixarenes as selective receptors continues to be

G. L. Nealon · M. Mocerino · M. I. Ogden (✉)
Nanochemistry Research Institute, Department of Chemistry,
Curtin University of Technology, GPO Box U 1987, Perth,
WA 6845, Australia
e-mail: m.ogden@curtin.edu.au
URL: http://www.chemistry.curtin.edu.au

B. W. Skelton
Chemistry M313, School of Biomedical, Biomolecular and
Chemical Sciences, University of Western Australia, Crawley,
WA 6009, Australia

an area of significant activity [1–4]. Amongst the many exotic elaborations on the basic calixarene macrocycle, simple alkylation of the lower rim O atoms with pendant donor atoms is a straightforward approach to modifying the selectivity of the receptor [5]. We have previously reviewed the structural chemistry of complexes of calixarenes substituted at the lower rim by amide moieties [6], where we also reported the structural analysis of the gadolinium complex of 5,11,17,23-tetra-*tert*-butyl-24-hydroxy-26,27,28-tris(diethylcarbamoylmethoxy)calix[4]arene (**L**). This tris-substituted calix[4]arene has seven O donor atoms available to the metal centre, leaving one to three coordination sites available about the lanthanide, which are typically (but not exclusively) 8-, 9- or 10-coordinate [7]. In the case of the complex [(pic-*O*)Gd{(**L**–H)(EtOH)}](pic)·2 EtOH [6] the coordination sites left vacant by the calixarene are filled by a *quasi*-bidentate picrate anion, with one O-nitro atom at a distance significantly longer than the phenolate-O atom. We report here the structural analysis of three additional lanthanide complexes of **L**, carried out to determine if a reduction in the metal ion radius, which might be expected to increase the crowding about the "vacant" coordination site, leads to a change in the binding of picrate anion.


L
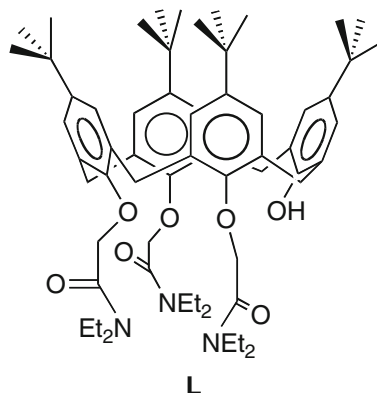
Experimental

Infrared spectra of the complexes were obtained with a PerkinElmer Spectrum 100 FT-IR spectrometer using the ATR technique.

Synthesis

5,11,17,23-Tetra-*tert*-butyl-24-hydroxy-26,27,28-tris(diethylcarbamoylmethoxy)calix[4]arene (**L**) was prepared as described previously [8]. The lanthanide picrate salts were prepared as described by Harrowfield et al. [9].

The general procedure employed to prepare the complexes was to add approximately three molar equivalents of the appropriate lanthanide picrate hydrate (ca. 15 mg, 15 μmol) to a solution of the calixarene **L** (5 mg, 5 μmol) in dichloromethane/ethanol (50:50 v/v, 2 mL). Crystals suitable for single crystal X-ray diffraction studies were deposited upon slow evaporation of the solvent over a number of days. The complexes were dried under vacuum prior to their analysis by infrared spectroscopy, causing desolvation of the crystals to give powders.

$[(pic\text{-}O)Sm\{(L\text{-}H)(EtOH)_{0.5}(CH_2Cl_2)_{0.5}\}](pic)\cdot EtOH\cdot 2H_2O$
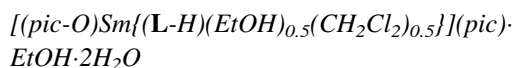
Dissolution of $[Sm(pic)_2(OH_2)_6](pic)\cdot 6H_2O$ and **L** in dichloromethane/ethanol produced an orange–yellow solution which deposited orange rhombic crystals after slow evaporation of the solvent.

IR (ATR, cm^{-1}), 1638 ν(C=O); 1574, 1546 ν_{as}(–NO$_2$); 1361, 1321 ν_s(–NO$_2$).

$[(pic\text{–}O)Ho\{(L\text{–}H)(CH_2Cl_2)\}](pic)\cdot(EtOH)$

Dissolution of $[Ho(pic)(OH_2)_7](pic)_2\cdot 4.5H_2O$ and **L** in dichloromethane/ethanol produced an orange–yellow solution which deposited orange rhombic crystals after slow evaporation of the solvent.

IR (ATR, cm^{-1}), 1635 ν(C=O); 1576, 1547 ν_{as}(–NO$_2$); 1362, 1325 ν_s(–NO$_2$).

$[(EtO\text{-}H)Yb\{(L\text{–}H)(EtOH)\}](pic)_2$
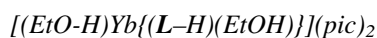
Dissolution of $[Yb(pic)(OH_2)_7](pic)_2\cdot 4.5H_2O$ and **L** in dichloromethane/ethanol produced a yellow solution which deposited yellow needlelike crystals after slow evaporation of the solvent.

IR (ATR, cm^{-1}), 1638 ν(C=O); 1557 ν_{as}(–NO$_2$); 1363, 1330 ν_s(–NO$_2$).

Structure determinations

The crystal data for Sm**L**, Ho**L** and Yb**L** are summarized in Table 1 with the structures depicted in Figs. 1, 2, and 3 where ellipsoids have been drawn at the 50% probability level. Selected coordination geometries are shown in Table 2. Crystallographic data for the structures were collected at 100(2) K on an Oxford Diffraction Gemini diffractometer fitted with graphite-monochromated Mo Kα radiation yielding N_{total} reflections, these merging to N unique after multi-scan absorption correction (maximum and minimum transmission coefficients, $T_{max,min}$ and R_{int} cited), with N_o reflections having $I > 2\sigma(I)$. The structures were refined against F^2 with full-matrix least-squares using the program SHELXL-97 [10]. All H-atoms, unless otherwise specified, were added at calculated positions and refined by use of a riding model with isotropic displacement parameters based on the isotropic displacement parameter of the parent atom.

Variata

Sm**L**: The C atoms of one methyl group (C24n) are disordered over two sets of sites with site occupancy factors refined to 0.715(10) and 1–0.715(10). These atoms and those of one solvent ethanol molecule were refined with isotropic displacement parameters. The solvent in the cavity was modelled as being part CH$_2$Cl$_2$ and part EtOH with site occupancy factors set at 0.5 for each after trial refinement. Two other peaks in the later difference maps were assigned as O atoms of water molecules. Solvent sites were found to be fully occupied. The H atoms on O atoms in ethanol and water molecules were not located. The overall formula is therefore $[C_{62}H_{88}N_3O_7Sm]^+$, picrate$^-$, $1/2(CH_2Cl_2)$, $3/2(C_2H_5OH)$.

Ho**L**: The methyl groups of two NEt$_2$ moieties were modelled as being disordered over two sites, the site occupancy factors being set at 0.5 after trial refinement.

Yb**L**: The hydroxyl H atom of the coordinated EtOH molecule was refined with restrained geometries.

Results and discussion

Samarium, holmium and ytterbium complexes of **L** were readily synthesised as described previously for gadolinium [6], with no notable differences in the synthetic procedures used. For the lighter lanthanides (including gadolinium) a distinct change from the yellow colour typical of the metal picrates to a darker orange was observed in solution, ultimately producing orange crystals. In the case of ytterbium, however, no change in the colour of the solution could be discerned by eye, and the yellow crystals finally obtained

Table 1 Crystal data for the structures SmL, HoL, and YbL

	SmL	HoL	YbL
Empirical formula	$C_{77.50}H_{106}ClN_9O_{24.50}Sm$	$C_{77}H_{100}Cl_2HoN_9O_{22}$	$C_{78}H_{104}N_9O_{23}Yb$
Formula weight	1741.51	1739.49	1708.74
Crystal system	Triclinic	Triclinic	Monoclinic
Space group	$P\bar{1}$	$P\bar{1}$	$P2_1/n$
T (K)	100(2)	100(2)	100(2)
a (Å)	12.6760(6)	12.6602(6)	13.2418(2)
b (Å)	14.4515(6)	14.4506(4)	27.8254(7)
c (Å)	24.602(1)	23.4573(8)	22.3540(9)
α (°)	102.548(3)	72.185(2)	90
β (°)	94.719(4)	79.703(2)	91.571(2)
γ (°)	105.720(4)	89.728(3)	90
V (Å^3)	4186.6(3)	4014.2(3)	8233.4(4)
Z	2	2	4
ρ (g cm^{-3})	1.381	1.439	1.378
μ (mm^{-1})	0.812	1.131	1.214
'T'$_{max/min}$	1.0/0.90	0.89/0.77	0.88/0.83
Crystal size (mm)	$0.17 \times 0.14 \times 0.03$	$0.17 \times 0.11 \times 0.10$	$0.27 \times 0.11 \times 0.11$
θ_{max} (°)	31.6	30.74	30.75
N_{total}	47529	42421	90496
N	24860	21761	23407
R_{int}	0.064	0.0569	0.0785
N_o	14923	13678	15106
Data/restraints/parameters	24860/0/1056	21761/0/1029	23407/2/1025
G.O.F. (F^2)	0.934	0.836	0.994
R_1, wR_2 [$I > 2\sigma(I)$]	0.0569, 0.1255	0.0455,0.0637	0.0624,0.131
R_1, wR_2 [all data]	0.1073, 0.1421	0.0885, 0.0696	0.118, 0.154
$\Delta\rho$(max, min) (e.Å^{-3})	2.63, −1.12	1.754, −1.085	2.677, −1.265

were of a similar colour to the ytterbium picrate starting material. Information regarding the coordination environment of the metal ion in the solid state was obtained by examining the infrared spectra of the complexes using the ATR technique. The $v_{as}(-NO_2)$ appears as two bands at 1574 and 1546 cm^{-1} for SmL and 1576 and 1547 cm^{-1} for the HoL complex, which is consistent with a coordinated picrate anion [11]. In contrast, the $v_{as}(-NO_2)$ appears as a single band at 1557 cm^{-1} for the YbL complex, which perhaps suggests that the picrate anions are not involved in coordination to the metal.

We have reported previously the structural analysis of the gadolinium complex (GdL) of **L**, formulated as [(pic-O)Gd{(**L**–H)(EtOH)}](pic)·2EtOH [6]. Details of the structural analyses of the three complexes reported here are given in Table 1. The complex of samarium (Fig. 1) was found to be isomorphous with the Gd complex, albeit with some differences in the model found to best fit the (inevitably somewhat poorly defined) solvent molecules. Thus, the samarium complex (SmL) is formulated as [(pic-O)Sm{(**L**–H)(EtOH)$_{0.5}$(CH$_2$Cl$_2$)$_{0.5}$}](pic)·EtOH·2H$_2$O, the

solvent occupying the calixarene cavity being modeled as part dichloromethane, part ethanol. The holmium complex (HoL), while similar to these two structures, is not isomorphous, and is formulated as[(pic-O)Ho{(**L**–H)(CH$_2$Cl$_2$)}](pic)·EtOH (Fig. 2). A significant structural change is found with the ytterbium complex (YbL), as was anticipated based on the colour change and IR spectroscopic results discussed above. The picrate anion is now excluded from the first coordination sphere and replaced with a solvent ethanol molecule, leading to a formulation of [(EtOH)Yb{(**L**–H)(EtOH)}](pic)$_2$ (Fig. 3a).

Some of the important structural parameters of the complex cations are given in Table 2. The calixarene Ln–O distances decrease essentially monotonically across the series as expected with decreasing metal atom radius, as do the picrate phenol-O distances (noting that for YbL, the additional ligand is ethanol, rather than picrate). Conversely, the closest approach of a nitro-O atom increases with decreasing lanthanide radius, such that the *quasi*-bidentate picrate observed for the Sm and Gd complexes becomes quite clearly unidentate for HoL. The Sm and Gd
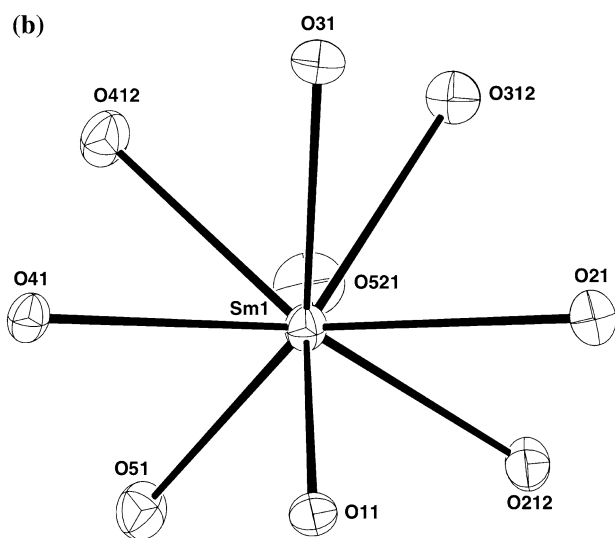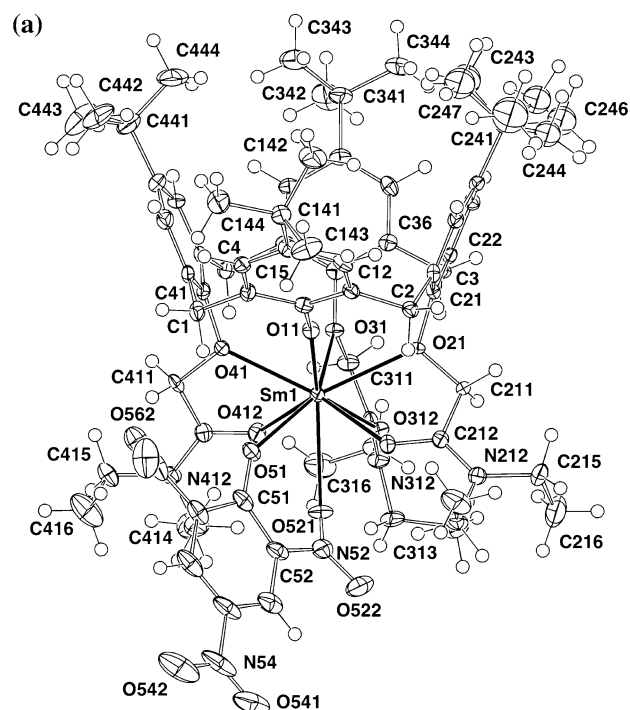
(a)

(b)

Fig. 1 **a** The structure of the complex cation of Sm**L**, and **b** the coordination sphere of the Sm atom

Fig. 2 The structure of the complex cation of Ho**L**

atoms are therefore nine-coordinate and can be viewed as a distorted capped square antiprism with the four phenolic O atoms forming one plane, and the three amide O atoms and O51 forming the second plane of the anti-prism with the capping atom for Sm**L** being O521 as shown in Fig. 1b. The coordination environment around the 8-coordinate Ho atom can be considered as a distorted square antiprism. It is tempting to ascribe this trend to increasing steric demand of the calixarene ligand around the smaller metal atom, and indeed this may be the case. It should be noted that a similar transition from bidentate to unidentate is observed
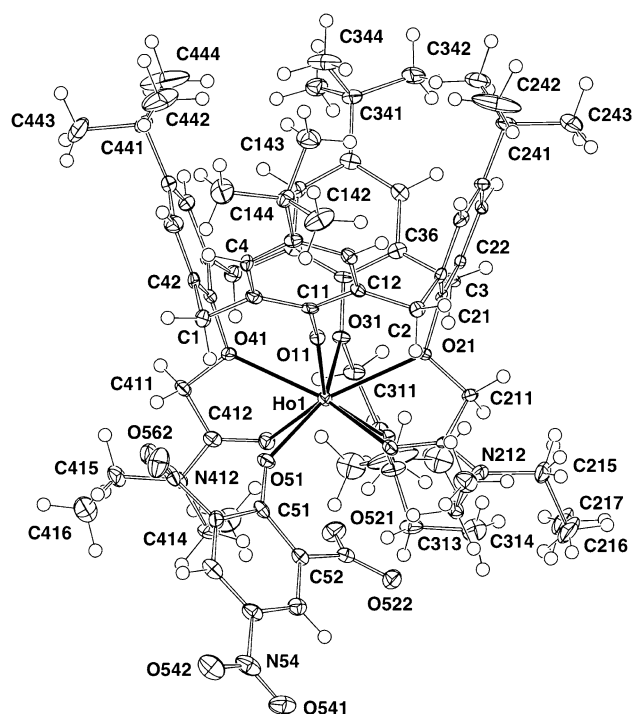
in the "simple" lanthanide picrate hydrates [9, 12] albeit with some complicating issues associated with the isolation of different phases with the same lanthanide [13, 14]. There are, however, examples of bidentate picrate–holmium interactions, and hence it is difficult to draw any specific conclusions from these observations [15]. If one considers the disposition of the amide moieties, as illustrated by the C(n1)–O(n1)–C(n11)–C(n12) torsion angles (Table 3), the twist of the $n = 2$ group that enables access of the picrate anion (as noted in previous work [6]) is actually increased in the holmium complex (corresponding to a reduction in the torsion angle), suggesting that the steric demands of the picrate anion are increased relative to Sm**L** and Gd**L**, despite the change to unidentate binding. The significant change in this torsion in Yb**L**, where the less sterically demanding ethanol ligand is found, also supports the hypothesis that the steric crowding in Ho**L** is the origin of the change in the picrate binding mode.

Continuing the reduction in lanthanide radius in Yb**L**, it is perhaps unsurprising given the discussion above, that picrate can no longer be accommodated in the primary coordination sphere in this complex. The metal centre remains 8-coordinate by virtue of a solvent ethanol ligand, and can still be considered as a distorted square antiprism. It is notable that a picrate anion is now located in the second coordination sphere of the Yb centre, with a close approach between ethanol OH and the phenol O atom of the picrate anion (O(201)···O(51), 2.711 Å) consistent with the presence of a hydrogen bond (Fig. 3b). In all three
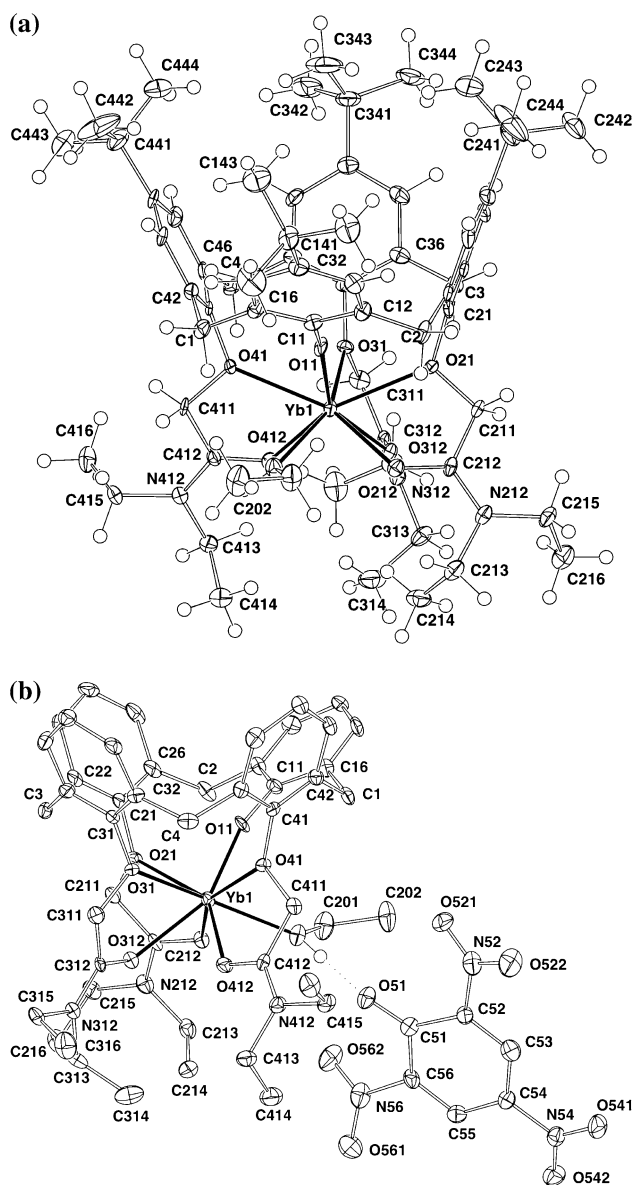
(a)

(b)

Fig. 3 a The structure of the complex cation of Yb**L**, and **b** the complex cation with picrate anion in the second coordination sphere, through an H-bond with the ethanol ligand. ᵗBu C and C–H H atoms have been removed for clarity

Table 2 Selected bond lengths [Å] and angles [deg]

	Sm**L**	Gd**L**[a]	Ho**L**	Yb**L**
Phenol O				
Ln–O(11)	2.148(3)	2.132(3)	2.093(2)	2.059(3)
Ln–O(21)	2.589(2)	2.576(2)	2.535(2)	2.490(3)
Ln–O(31)	2.647(3)	2.618(2)	2.593(2)	2.488(3)
Ln–O(41)	2.516(2)	2.510(3)	2.488(2)	2.469(3)
Amide O				
Ln–O(212)	2.428(3)	2.398(2)	2.342(2)	2.289(2)
Ln–O(312)	2.384(3)	2.369(2)	2.329(2)	2.322(3)
Ln–O(412)	2.428(3)	2.414(3)	2.366(2)	2.316(3)
Picrate O				
Ln–O(51)	2.417(3)	2.371(2)	2.291(2)	2.332(3)[b]
Ln–O(521)	2.773(3)	2.799(4)	3.107(2)	–

[a] From reference [6]

[b] Yb–O(201) distance (ethanol O atom)

Table 3 Torsion angles C(*n*1)–O(*n*1)–C(*n*11)–C(*n*12) (deg)

n	Sm**L**	Gd**L**[a]	Ho**L**	Yb**L**
2	132.5	132.2	128.1	145.5
3	156.7	157.0	153.1	157.5
4	157.3	157.2	159.9	157.3

[a] From [6]

incorporated solvent molecules depends on subtle changes in the solvent composition when crystallisation occurs.

Work is now underway to extend these studies to the complete lanthanide series, to further investigate the structural changes as a function of the lanthanide cation radius.

Supplementary material

Full details of the structure determinations for the compounds Sm**L**, Ho**L**, Yb**L** have been deposited with the Cambridge Crystallographic Data Centre as **CCDC** 730781, 730782, and 730783. These data can be obtained free of charge via http://www.ccdc.cam.ac.uk/conts/retrieving. html, or from the Cambridge Crystallographic Data Centre, 12 Union Road, Cambridge CB2 1EZ, UK; fax: (+44) 1223-336-033; or e-mail: deposit@ccdc.cam.ac.uk.

References

1. Harrowfield, J., Vicens, J.: New trends in calixarene chemistry—preface. Tetrahedron **63**, 10719 (2007)
2. Asfari, Z., Böhmer, V., Harrowfield, J.M., Vicens, J. (eds.): Calixarenes 2001. Kluwer, Dordrecht (2001)

structures, the five membered chelates formed by the amide arms are twisted to define a chiral complex, with adjacent complexes alternating between the two enantiomers.

A solvent molecule is located in the cavity defined by the four phenyl rings of the calixarene in all of these structures. The solvent in Sm**L** was modelled as disordered ethanol and dichloromethane at 0.5 occupancy for each component. The Gd**L** complex was found to have an ethanol molecule in the cavity, as was Yb**L**. In contrast, the solvent in the cavity of Ho**L** was best modelled as a molecule of dichloromethane. No obvious trend emerges from these observations, and it is possible that the nature of the

3. Gutsche, C.D.: Calixarenes Revisited. The Royal Society of Chemistry, Cambridge (1998)
4. Vicens, J., Harrowfield, J.M. (eds.): Calixarenes in the Nanoworld. Springer, Dordrecht (2006)
5. Creaven, B.S., Donlon, D.F., McGinley, J.: Coordination chemistry of calix[4]arene derivatives with lower rim functionalisation and their applications. Coord. Chem. Rev. **253**, 893–962 (2009)
6. Ogden, M.I., Skelton, B.W., White, A.H.: Synthesis and structural studies of a lanthanide complex of a calix[4]arene trisamide. C.R. Chim. **8**, 181–187 (2005)
7. Harrowfield, J.M.: Biologically relevant structural coordination chemistry of simple lanthanide ion complexes. Met. Ions Biol. Syst. **40**, 105–159 (2003)
8. Ogden, M.I., Skelton, B.W., White, A.H.: Syntheses, structural studies and solution properties of iron complexes of some amide-substituted calixarenes. J. Chem. Soc. Dalton Trans. 3073–3077 (2001)
9. Harrowfield, J.M., Lu, W.M., Skelton, B.W., White, A.H.: Structural systematics of rare earth complexes. I. Structural characterization of lanthanoid(III) picrate hydrates: monoclinic (P2(1)/c) quasi-dodecahydrates of the related La–Pr and Nd–Tb families. Aust. J. Chem. **47**, 321–337 (1994)
10. Sheldrick, G.M.: SHELXL-97. Acta Cryst. **A64**, 112–122 (2008)
11. Bermudez, V.D., Carlos, L.D., Silva, M.M., Smith, M.J.: An interesting ligand for the preparation of luminescent plastics: the picrate ion. J. Chem. Phys. **112**, 3293–3313 (2000)
12. Harrowfield, J.M., Lu, W.M., Skelton, B.W., White, A.H.: Structural systematics of rare earth complexes. II. Structural characterization of lanthanoid(III) picrate hydrates: the triclinic P1, 11.5 hydrates of the later rare earths and yttrium. Aust. J. Chem. **47**, 339–348 (1994)
13. Harrowfield, J.M., Lu, W.M., Skelton, B.W., White, A.H.: Structural systematics of rare earth complexes. III. Structural characterization of lanthanoid(III) picrate hydrates: gadolinium picrate dodecahydrate; an X-ray-induced phase modification; and some general aspects of the structural chemistry of lanthanoid picrates. Aust. J. Chem. **47**, 349–358 (1994)
14. Harrowfield, J.M., Skelton, B.W., White, A.H.: Structural systematics of rare earth complexes. IV. Structural characterization of lanthanoid(III) picrate hydrates: the quasi-undecahydrate of samarium(III) picrate. Aust. J. Chem. **47**, 359–364 (1994)
15. Saleh, M.I., Kusrini, E., Fun, H.K., Yamin, B.M.: Structural and selectivity of 18-crown-6 ligand in lanthanide-picrate complexes. J. Organomet. Chem. **693**, 2561–2571 (2008)